Image Cover Sheet

CLASSIFICATION	SYSTEM NUMBER
UNCLASSIFIED	498353

TITLE

NUMERICAL DEVELOPMENT O AN EQUIVALENT AXISYMMETRIC RAGMENT SIMULATING PROJECTILE

System Number:

Patron Number:

Requester:

Notes:

DSIS Use only:

Deliver to:

DEFENCE RESEARCH ESTABLISHMENT
CENTRE DE RECERCHES POUR LA DÉFENSE
VALCARTIER, QUÉBEC

DREV - R-9530

NUMERICAL DEVELOPMENT OF AN EQUIVALENT AXISYMMETRIC FRAGMENT SIMULATING PROJECTILE

by

D. Nandlall

March/mars 1996

Approved by/approuvé par

Chief Scientist/Scientifique en chef

27 March 96

Date

ABSTRACT

In this study, an attempt is made to develop an equivalent axisymmetric fragment simulating projectile (FSP) to represent a nonaxisymmetric standard FSP for the development of calibration curves for witness packs, using numerical simulations. Three different axisymmetric FSP models were investigated. In the first model, the cutting edge perimeter of the true FSP was conserved. For the second model, the presented area of the true FSP on impact was conserved. For the third model, the bevel angle was conserved. The results obtained indicate that the third model yields the same ballistic limit as the standard nonaxisymmetric FSP. However, it was found that the plug formation modes for the axisymmetric and nonaxisymmetric models differ substantially.

RÉSUMÉ

Dans cette étude, on utilise une simulation numérique par hydrocode afin de trouver un équivalent axisymétrique au projectile simulateur de fragment (PSF). Ce nouveau projectile sera utilisé pour l'étalonnage des panneaux témoins d'effets arrière. Trois modèles sont évalués: le premier respecte le périmètre de l'arête du PSF standard, le deuxième conserve la surface présentée et le troisième l'angle de chanfrein. Les résultats montrent que le troisième modèle a la même limite balistique que le PSF simulé. Cependant, le processus de formation de la rondelle ("plug") est différent.

TABLE OF CONTENTS

EXECUTIVE SUMMARY

The ability to predict the penetration of a target by a projectile is of fundamental importance for military applications. Consequently, considerable resources have been devoted to the development of expensive empirical methods and experimental testing to predict and measure residual velocities which are crucial to the accuracy of many vulnerability studies.

A conventional approach to the determination of fragment residual velocities is to launch pre-formed fragments or fragment simulating projectiles (FSP) at various targets, such as witness packs, and measure both the striking and residual velocities. Witness packs are used to study the effects of behind-armour debris and to obtain threat/armour interaction data for vulnerability/lethality studies. For reliable interpretation of witness pack data, the witness pack must be calibrated to find the threshold energy for each plate within the pack. This threshold energy is the minimum energy required by a fragment of a particular mass to perforate the plate. Since it requires between 250 to 300 firings to calibrate a simple 4-plate witness pack using four similar FSPs each of different mass, it can be seen that the experimental calibration of a witness pack is a time consuming and extremely expensive process .

At Defence Research Establishment Valcartier, an alternative approach to the calibration of witness packs by numerical simulation with a hydrodynamic finite element code and a limited number of experiments is being developed. However, since the standard FSPs are not axisymmetric, 3D simulations have to be performed to represent accurately the geometry of the FSP. A major disadvantage in the use of 3D simulations is the large amount of CPU time required to simulate the penetration process accurately . On the other hand, a 2D hydrocode performs the same simulations in a substantially shorter CPU time. An axisymmetric FSP that yields the same ballistic limit as the standard non-axisymmetric FSP is however required.

The study presented in this report examines the possibilities of developing an equivalent axisymmetric FSP to conduct 2D hydrocode simulations. Three different axisymmetric FSPs were investigated and it was found that in the case where the bevel angle of the non-axisymmetric FSP was conserved, the ballistic limit curve matches quite closely that of the true FSP. From the results presented it was concluded that for the purpose of obtaining the ballistic limit, an axisymmetric FSP and a 2D hydrocode is adequate and yields considerable savings in CPU time and consequently experimental tests.

1.0 INTRODUCTION

In recent years, researchers have been developing many methods to record behind-armour debris data in order to better analyze the effectiveness of a weapon system or the vulnerability of a target. One such method is the use of metallic witness packs behind the target to capture the behind-armour debris. Figure 1(a) shows a typical metallic witness pack constructed of three aluminium and one steel plates. The principle of the witness pack is that it acts as an energy sieve with each plate in the pack corresponding to a discrete energy level. This experimental method has proven itself to be a cost-effective means of recording behind armour debris.

For reliable interpretation of witness pack data, the witness pack must be calibrated to find the threshold energy for each plate. This threshold energy is the minimum energy required by a fragment of a particular mass to perforate the plate. Figure 1(b) shows a typical standard fragment simulating projectile (FSP). Such FSPs can be used to calibrate witness packs experimentally. Normally, a variety of FSPs with basically the same nose shape but different masses is used to represent the various masses of fragments in behind-armour debris. In order to experimentally calibrate a witness pack, the limit velocity of each FSP for each plate must be known. This experimental process is time-consuming and expensive since it requires between 250 to 300 firings to calibrate a simple 4-plate witness pack with four similar FSPs, each of a different mass.

An alternative approach that is currently under investigation is to calibrate the witness packs by numerical simulation by means of a hydrodynamic finite element code and a limited number of experiments. However, the standard FSP is not axisymmetric and 3D simulations have to be performed to acurately represent the geometry of the FSP. A major disadvantage in the use of 3D simulations is that,

because of the number of elements required to simulate accurately the penetration process, 15 hours of CPU time on an INDIGO 2 (MIPS 4400 processor) workstation are required to complete a simulation of a standard 44-grain FSP impacting a three-plate witness pack. The CPU time increases significantly with the number of plates. A 2D hydrocode can perform the same simulations in a shorter CPU time because it requires fewer elements. However, to perform 2D simulations, an equivalent axisymmetric FSP is required to represent the standard non-axisymmetric FSP. The study presented in this report examines the possibilities of developing an equivalent axisymmetric FSP and was done at the Defence Research Establishment Valcartier (DREV), under PSC 32G between December 1994 and May 1995.

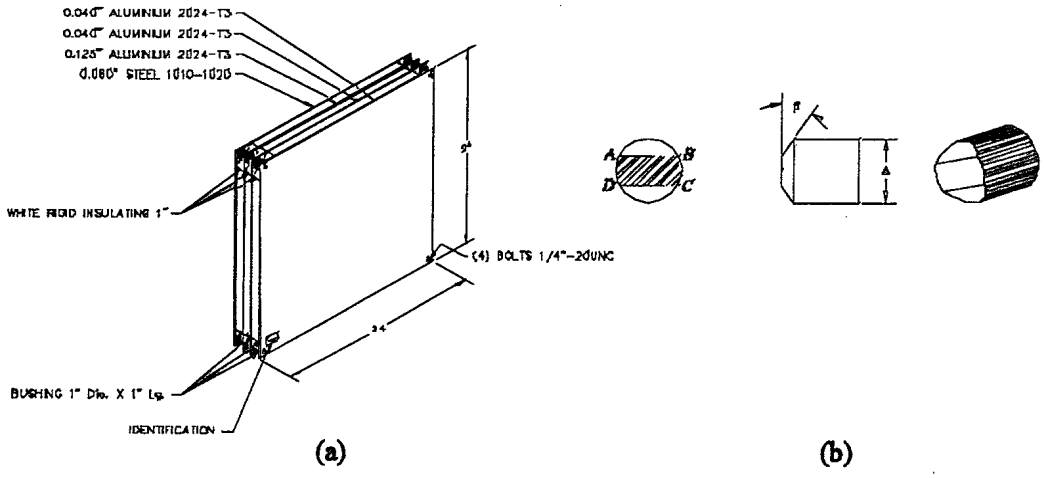

FIGURE 1 - (a) Typical Aluminium/Steel witness pack
(b) Standard Fragment Simulating Projectile (FSP)

2.0 OBJECTIVE

An experimental programme is in progress at DREV to study and evaluate the ballistic behaviour of behind armour debris (Refs. 1 and 2). This study is conducted using metallic witness packs and a variety of FSPs representing a wide range of behind armour debris. However, to interpret witness pack data the witness packs must

be calibrated. As discussed in the previous section, this calibration is quite expensive using experimental methods or 3D hydrocode simulations.

The primary objective of the present work is to use 3D hydrocode simulations to develop an equivalent axisymmetric FSP which would give the same ballistic performance as the standard non-axisymmetric FSPs which are used in the experimental programme.

A second objective of the work is to examine and compare the crater development and the plug formation for the standard non-axisymmetric FSP and the equivalent axisymmetric FSP developed.

3.0 PROJECTILE AND TARGET DESCRIPTION

Figure 2 shows the main features and differences in the geometries of the true and modelled FSPs used in this study. Figure 2(a) shows the standard non-axisymmetric FSP with a length to diameter ratio of 1.176. The rectangle ABCD indicates the cutting perimeter and the shaded region shows the presented area of the FSP on impact. A modified axisymmetric FSP for which the cutting perimeter of the standard FSP is conserved is shown in Fig. 2(b). Figure 2(c) shows another equivalent axisymmetric FSP for which, in contrast, the presented area ABCD of the standard FSP is conserved. Figure 2(d) shows an equivalent axisymmetric FSP for which the bevel angle, β, of the standard FSP is conserved. The parameters describing the four types of FSP used in this study are given in Table I. From these parameters it can be observed that the equivalent FSPs have between 1.5 and 0.5 % lower masses than that of the true FSP. This small difference is more than acceptable since these variations translate to less than 1.5% lower impact kinetic energy for the equivalent FSPs in the worst case situation.

TABLE I

Fragment simulating projectiles (FSPs) parameters

Fragment Type	L/D	d_e (cm)	Mass (g)
FSP_{std}	1.176	-	2.947
FSP_{peri}		0.6536	2.946
FSP_{area}		0.5645	2.896
FSP_{ang}		0.4064	2.944

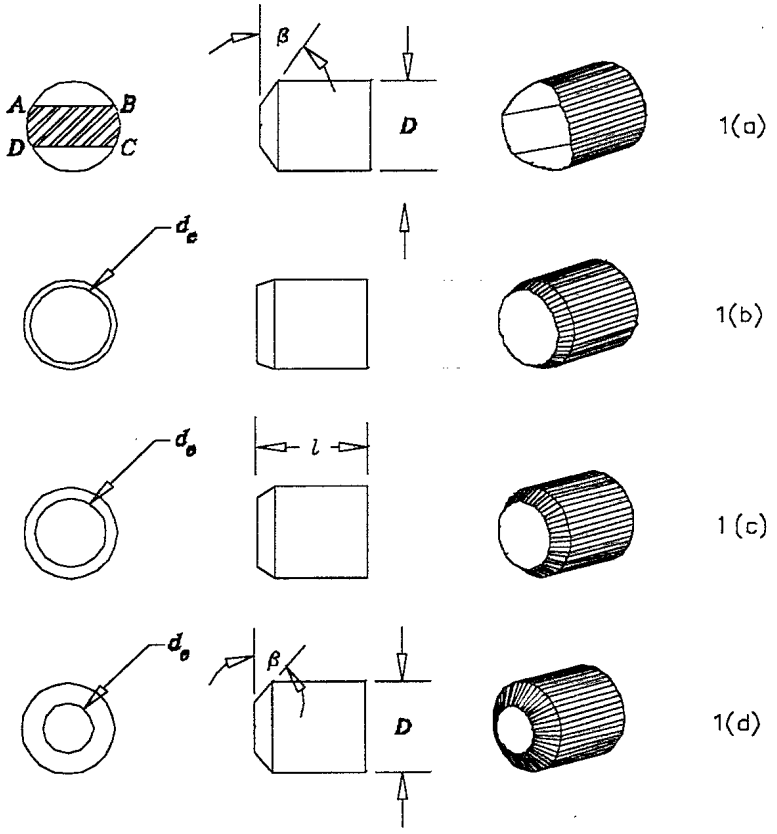

FIGURE 2 - Standard non-axisymmetric and equivalent axisymmetric FSP geometries

The target used in this study is a 3/8-inch thick 2024-T3 aluminium plate which represents the first plate of a typical witness pack currently used at DREV. This witness pack meets the STANAG 4190 specifications.

4.0 NUMERICAL SIMULATIONS

LS-DYNA3D (Ref. 3), a hydrodynamic computer code, was applied to the problem of simulating the penetration process of various FSPs striking a single aluminium plate at different impact velocities. The LS-DYNA3D hydrocode is an explicit two-dimensional lagrangian finite element code used for analyzing the large deformation and high strain rate response of inelastic solids and structures.

4.1 Numerical Mesh

To model the impact, penetration and deformation which occurs when the projectile strikes a target, and the subsequent deformation of the target, it is necessary to divide the FSP and the target plate into a finite number of regions called elements. The network of elements obtained is called a mesh. The computation is then performed by solving the constitutive equations for the distortion of the invidual elements within the mesh. For the present study, the mesh was generated with the preprocessor LS/INGRID that generates three dimensional meshes for LSDYNA3D.

Figure 3 shows the initial global finite element mesh that was used as the "zero" time state for all the simulations. In this case the mesh represents the first plate of a witness pack being struck by the non-axisymmetric standard FSP shown in Fig. 2 (a). Due to the symmetric nature of the problem in two planes, only a quarter of the domain was simulated. This 3D quarter domain, shown in Fig. 3, consists of a total of 12948 brick elements of which 3828 are in the projectile and 9120 are in the target.

In order for the simulations to be realistic, the areas that experience large and intense deformation must be finely gridded to minimize the overlapping of the projectile and target elements during the penetration process. It is in this region where the high rates of stress change and large deformations occur. A coarse geometric mesh was constructed at the outer part of the geometry to reduce the CPU execution time required to complete a simulation. This coarsely meshed region is sufficient for this particular target/projectile combination because the high rates of deformation were constrained to within 0.5-projectile diameter from the projectile/target interface. There are no relatively high rates of deformation in the coarsely meshed region. A simplified sensitivity analysis of the mesh was also performed. In this analysis, simulations were performed with different mesh densities to arrive at the optimum meshing that was used in this study. A typical LS-INGRID file that was used to produce the meshes used in this study is given in Appendix A.

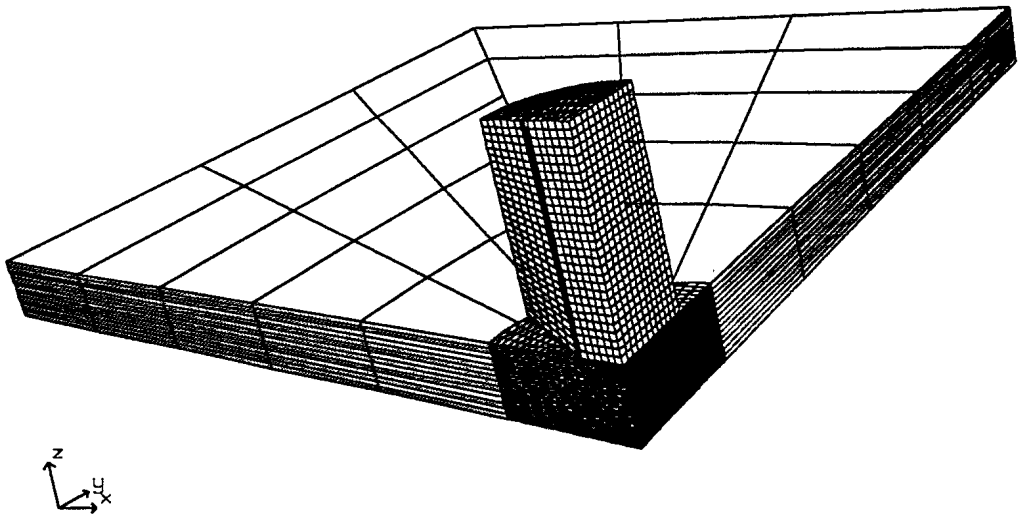

FIGURE 3 - Mesh of target and standard non-axisymmetric FSP

4.2 Material Models

To model the material behaviour in the hydrocode, two equations are normally used: a constitutive equation to describe the distortion of the material under stress; and the equation of state to describe the specific response of the material to volume changes with pressure. The constitutive equation is a functional relationship relating flow stress of a material to such parameters as strain, strain rate and temperature. The equation of state is a thermodynamic relation that compares or calculates the pressure, volume and a thermal parameter (internal energy or temperature).

For all the numerical simulations presented, the kinematic/isotropic elastic-plastic material model was used to model the FSPs since, based on the experimental results, the FSPs were not expected to deform. This model is a simplistic constitutive model material model which assumes a bi-linear stress-strain behaviour of the material neglecting the strain rate effects. The material properties used for the constitutive modelling of the FSPs are given in Table II.

The target was modelled using the hydrodynamic-elastic-plastic model, which is based on the same principle as the model used for the projectile. However, this model includes a pressure cut-off value and uses the effective plastic strain as the governing erosion parameter.This hydrodynamic-elastic-plastic model coupled with the erosion model provides realistic numerical predictions of a very broad class of applications involving extreme dynamic events such as impact, penetration and explosive acceleration of metallic materials. An alternative model which was considered is the Johnson-Cook model. However, even though this model is quite capable of producing very good numerical results, it was found that the model did not respond well to the erosion algorithm which is needed to conduct ballistic limit studies. The material properties used for the modelling of the target are also given in Table II.

TABLE II

Parameters used for hydrocode modelling

Material Property	Projectile (FSPs)	Target 2024-T3 Al	
Constitutive Model	Elastic-Plastic	Elastic-Plastic Hydrodynamic	Equation of State
ρ (g/cm^3)	7.8	2.768	Polynomial
E (Mbars)	2.068	0.7182	C_0=0.00
ν	0.30	0.33	C_1=0.75
ϵ	--	0.54	C_2=0.65
E_t (Mbars)	0.00685	0.006457	C_3=0.00
σ (Mbars)	0.010342	0.00335	C_4=2.13
β	1.0	1.0	C_5=2.13

5.0 COMPUTATIONAL RESULTS

In all the simulations performed a 3/8-inch aluminium plate was used as the target. Four different cases were studied. In the first case, simulations were performed using the standard non-axisymmetric FSP shown in Fig. 2(a). This was done to determine the ballistic limit of the true FSP against the target. This ballistic limit was then used as a baseline ballistic limit to compare the ballistic performance of the equivalent axisymmetric FSPs. For the second case, simulations were performed to obtain the ballistic limit of the target using the FSP shown in Fig. 2 (b) in which case the cutting edge perimeter of the true FSP was conserved. In the third case simulations were performed using the FSP shown in Fig. 2(c) where the presenting area of the true FSP as it struck the target was conserved. In the fourth case, similar simulations were performed using the FSP shown in Fig. 2(d). In this case, the bevel angle of the true FSP was conserved.

5.1 Ballistic Limit Determination

For the purpose of this study, the ballistic limit is defined as the minimum striking velocity required by the projectile to completely perforate the target and produce a behind target plug. This impact velocity is then called the V_{100} limit or the ballistic limit of target relative to the projectile used. Figure 4 shows an example of a typical simulation that was performed in an effort to obtain the ballistic limit.

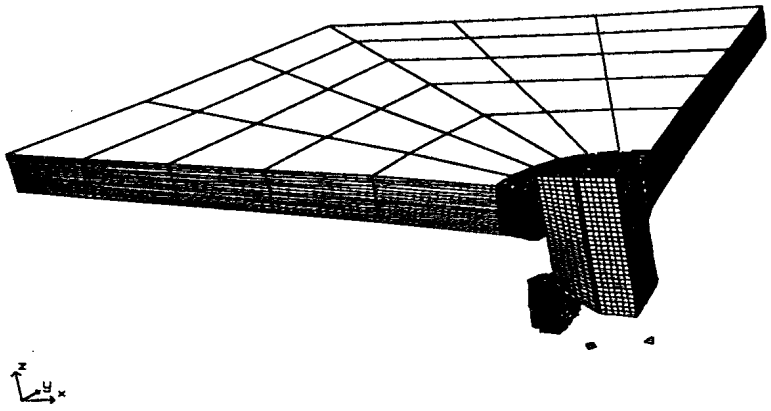

FIGURE 4 - Typical simulation performed to obtain ballistic limit of target

The technique used to obtain the V_{100} limit is to perform a simulation of an FSP at a striking velocity high enough to completely perforate the target. The residual velocity of the projectile as it exits the target is then measured. Successive simulations are then performed by reducing the striking velocity by about 5 to 10 m/s each time until there is no perforation of the target plate. The residual velocities are then plotted against the corresponding impact velocities and the V_{100} limit can be estimated by performing a non-linear regression fit to the numerical data. This method is discussed in detail by Zukas (Ref. 4). Figure 5 shows a typical non-linear regression fit performed on the numerical data to obtain the ballistic limit. In this particular case the ballistic limit for the standard FSP was found to be 195 m/s.

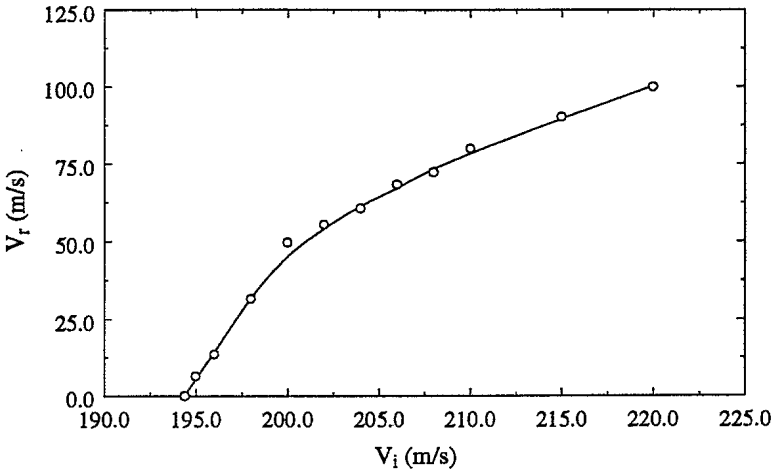

FIGURE 5 - Typical non-linear regression fit used for obtaining the V_{100} ballistic limit

Figure 6 shows the variation of the projectile velocity as a function of time for the various striking velocities used to obtained the ballistic limit using simulations on both sides of the ballistic limit. Careful observation of the velocity curves reveal that there is a time period, T_r, during which the projectile stays at the bottom of the crater before rebounding. As the impact velocity approaches the limit velocity, T_r approaches zero. This effect presents another way of observing and characterizing the ballistic limit.

Figure 7 shows the variation of the projectile displacement as function of time for different striking velocities for the standard FSP. Again, as in Fig. 6, it is possible to observe the effect of the ballistic limit. However, in this case the effect of the rest time T_r is not as obvious as shown in Fig. 6.

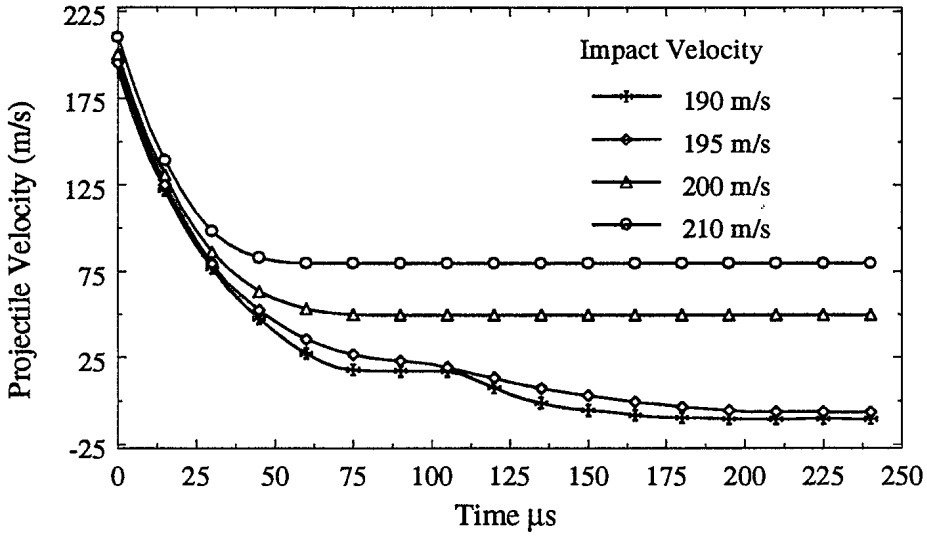

FIGURE 6 - Velocity variation as a function of time for the true FSP at different striking velocities

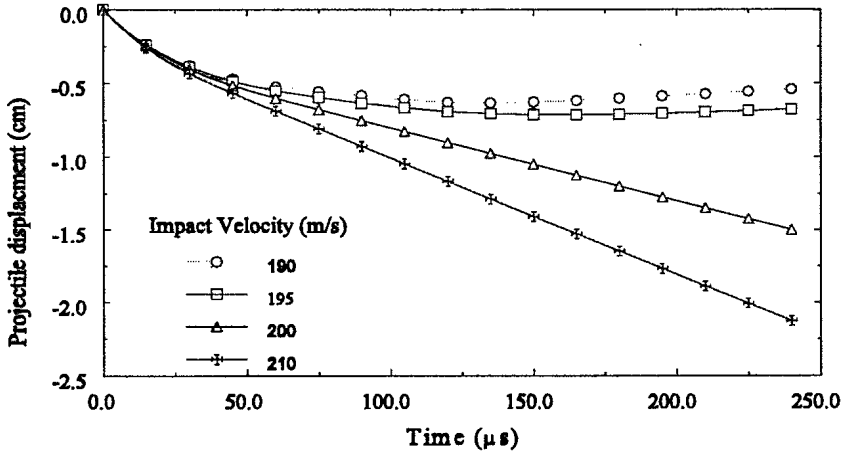

FIGURE 7 - Displacement variation as a function of time for the true FSP at various striking velocities

5.2 Ballistic Limits Comparison

Table III shows a comparison between the ballistic limits obtained for the standard and all equivalent axisymmetric FSPs shown in Fig. 2. As can be seen, the limit velocity for the case in which the bevel angle of the standard FSP was conserved approached that of the true FSP much more closely than the other two cases. These results seem to suggest that for equivalent masses the angle of the bevel of the equivalent FSP is the most important parameter in determining the ballistic limit of the target.

TABLE III

Ballistic limit comparisons between standard and equivalent FSPs

Fragment	Fragment Mass (g)	Ballistic Limit (m/s)
FSP_{std}	2.947	195
FSP_{peri}	2.946	176
FSP_{area}	2.896	184
FSP_{ang}	2.944	192

Figure 8 shows a comparison of the variation of the projectile velocity as a function of time for all the FSPs studied. The impact velocity in each case was the V_{100} limit velocity shown in Table III. From the curves shown, it can be seen clearly that the ballistic limit curve of the equivalent axisymmetric projectile, for an impact velocity of 192 m/s, matches the curve obtained for the standard non-axisymmetric FSP quite closely.

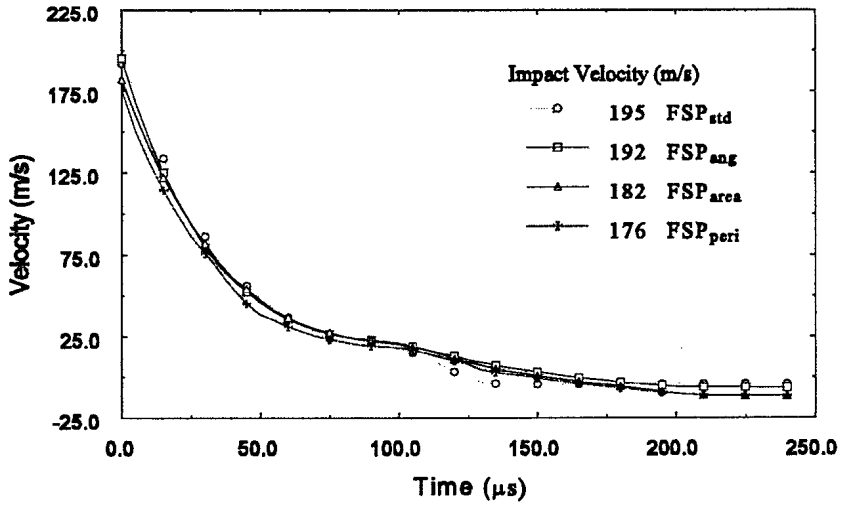

FIGURE 8 - Comparison of projectile velocity variation as a function of time for all FSPs

5.3 Plug and Crater Formation

Figure 9 (a) shows the crater and plug formation for the case of the equivalent axisymmetric FSP for which the bevel angle was conserved. Figure 9 (b) shows the crater and plug formation for the standard non-axisymmetric FSP. A comparison of the different plug formation in the two cases shows that, in the case of the axisymmetric FSP, the plug remains in front of the projectile after formation, while in the non-axisymmetric case the plug formation is such that the plug moves away from the projectile and target once it has been detached. The plug formation shown in Fig. 9 (a) is representative of the other axisymmetric models used in this study.

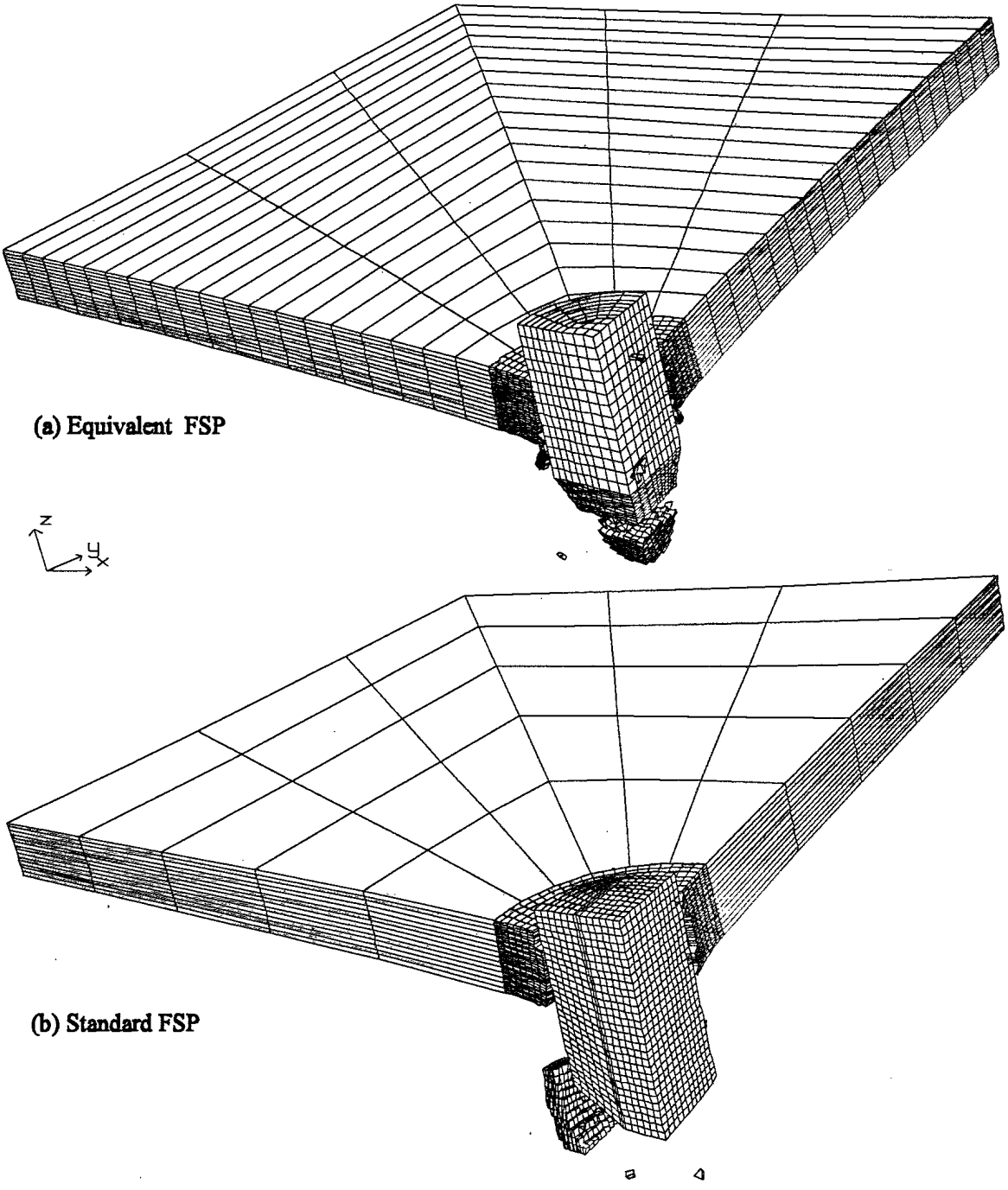

FIGURE 9 - Comparison of plug formation between the equivalent and standard FSPs

The difference in plug formation arises from the axisymmetric and non-axisymmetric nature of the FSPs presented surface on impact and penetration of the target. In the axisymmetric case, because the presented surface of the FSP is circular, the target material underneath the FSP shears off uniformly in all directions around the perimeter. As expected, the plug remains in front of the projectile. On the other hand, in the case of the non-axisymmetric FSP, the target material under the presented surface of the FSP first starts to shear around the circular portions of the perimeter. As the projectile continues to perforate the target, the plug moves away from the projectile because the bevel on the FSP forces the plug to rotate about the straight edge part of the perimeter. This indicates that the non-axisymmetric FSP can cause the plug to split into two pieces.

Since witness packs are multi-plate targets, this aspect of plug formation is important because the ballistic limit obtained can depend on whether the plug from the first plate penetrates the second or subsequent plates before the FSP does. If the plug penetrates the target before the FSP, the ballistic limit can be underpredicted since the residual velocity of the plug is usually higher than that of the projectile. This effect will be more significant for the smaller FSPs since the plug and the FSP masses are comparable.

6.0 CONCLUSIONS AND REMARKS

Using 3D hydrocode simulations, three different equivalent axisymmetric FSPs were investigated in an effort to find one that could represent a standard non-axisymmetric FSP.

It has been shown that, in the case for which the bevel angle of the non-axisymmetric FSP was conserved, the equivalent axisymmetric FSP yields a ballistic limit quite close to that of the true non-axisymmetric FSP. It was also shown that the plug formation mechanism for the equivalent axisymmetric FSP is different than that of the non-axisymmetric FSP and that, if the crater development in the target is of interest, the true non-axisymmetric FSP must be modelled. However, given that within the hydrocode it is possible to control whether the plug penetrates the target or not, these results indicate that, for the purpose of obtaining the ballistic limit, an axisymmetric FSP and a 2D hydrocode is adequate and yields considerable savings in CPU time.

The primary objective of this work was to develop numerically an axisymmetric FSP that could be used with a 2D hydrocode to give the same ballistic limit as the standard non-axisymmetric FSP. The results obtained in this study are in good agreement with the preliminary experimental results. The ballistic limits obtained by the simulations should be verified by experiments before being accepted as accurate.

The results in this report also indicate that there is a major difference in the plug formation between the axisymmetric and non-axisymmetric cases. Another extension of this work, which is currently in progress, is to verify the mechanism of the plug formation experimentally. This is necessary to determine whether the plug of a particular plate in a witness pack contributes to the penetration of any subsequent plate that follows or not.

7.0 ACKNOWLEDGEMENTS

The author would like to thank Messrs. M. Szymczak and G. Pageau for their advice and suggestions that helped in the development of the axisymmetric models. Thanks are also extended to Mr. R. Fiset for preparing the drawings of the FSPs and witness pack presented in this report. Special thanks are also extended to Dr. K. Heaton who took the time to review this document.

8.0 REFERENCES

[1] Nandlall, D.,"Numerical Comparison of a Standard FSP and an Equivalent Axisymmetric FSP for the Calibration of Witness Packs", Paper 15, Light Armour Systems Symposium '95, Royal Military College of Science, Shrivenham, England, 28-30 June 1995.

[2] Nandlall, D. et al., "The Numerical Development of Calibration Curves for Behind-Armour Debris Analysis", 15th Int. Symp. on Ballistics, Jerusalem, Israel, May, 1995.

[3] Hallquist, J., "LS-DYNA3D, User's Manual-Nonlinear Dynamic Analysis of Structures in Three Dimensions", LSTC Report 1007, Livermore Software Technology Corporation, Ca., USA, 1994.

[4] Zukas et al., "Impact Dynamics", Krieger Publishing Company, Malabar, Florida, USA, 1992.

APPENDIX A

INGRID INPUT FILE

```
Standard 44-g FSP
dn3d
v92
term 240.0 plti 5.0 prti 9999 newc
mat 1 type 3 ro 7.7504 e 2.06844 pr 0.3
   sigy 0.010342  etan .00685 endmat
mat 2 type 10
    ro 2.768 g 0.27 sigy 3.35e-3 eh 0.6457e-2 pc -.01125
     a1 0. a2 0. fs .338
    endmat
eos 1
    c0 0. c1 0.75 c2 .65 c3 0. c4 2.13 c5 2.13
    e0 0. v0 1.
    endeos
 plane 2
    0 0 0  0 1 0 .01 symm
    0 0 0 -1 0 0 .01 symm
si 1 tied ;
si 2 t14 material master 2 ; material slave 1 ; mpnl 5.0 spnl 0.1 ;
start
1 7 9 15 ; 1 7 13 ; 1  30;
-.2 -.2 -.17272 0. 0. .2 .2 0. .88392
di 1 2 ; 2 3 ; ;
sfi -1 4 ; 1 -3 ; ; cyli 0 0 0 0 0 1  .37592
pa 1 1 1 xz   -.17272 .14228
pb 3 3 1 3 3 2 xyz  -.17272 .33389 .0
```

```
sfi ; ; -2 ; plan 0 0 .88392 0 0 1
sfi 1 3 ; 1 3 ; -1 ; plan  -.17272 0 0  -.5736 0. -.8192
mate 1
velo 0 0 -.0199
end
 start
 1 11 21 31 41; 1 11 21 31 41; 1 30;
 -1.0 -1.0 0 1.0 1.0  -1.0 -1.0 0 1.0 1.0  0 -.3175
di 1 2 0 4 5 ; 1 2 0 4 5 ;  ;
sfi -1 -5 ; -1 -5 ; ; cy 0 0 0 0 0 1 0.6
sfvi -2 -4 ; -2 -4 ; ; cy 0 0 0 0 0 1 0.3
sii -1 -5 ; -1 -5 ; ; 1 s
 d 0 1 0 0 3 0
d 3 3 0 5 5 0
 mate 2
 end
start
1 6 9 12 17; 1 6 9 12 17; 1 15;
-4 -4 0 4 4 -4 -4 0 4 4 0 -.3175
di 1 2 0 4 5 ; 1 2 0 4 5; ;
d 2 2 0 4 4 0
sfi -2 -4 ; -2 -4 ; ; cy 0 0 0 0 0 1 0.6
sii -2 -4; -2 -4; ; 1 m
d 0 1 0 0 3 0
d 3 3 0 5 5 0
mate 2
end
end
```

INTERNAL DISTRIBUTION

DREV R-9530

1 - Deputy Director General
1 - Head, Weapon Effects
6 - Document Library
1 - D. Nandlall (author)
1 - R. Delagrave
1 - G. Pageau
1 - M. Bolduc
1 - B. St-Jean
1 - R. Fiset
1 - D. Leclerc

EXTERNAL DISTRIBUTION

DREV R-9530

2 - DSIS

1 - CRAD

1 - DSAL

1 - DSAL-2

1 - PMO LAV

1 - T. Wasmund, NSWC Dahlgren 8266

1 - R. Shnidman, ARL
Aberdeen Proving Ground 8244

2 - A. Poursartip and R. Vaziri
Metals and Materials Engineering 7004
University of British Columbia

1 - Dr. K. Heaton
DSTI, NDHQ

UNCLASSIFIED
SECURITY CLASSIFICATION OF FORM
(Highest classification of Title, Abstract, Keywords)

DOCUMENT CONTROL DATA

1. ORIGINATOR (name and address)	2. SECURITY CLASSIFICATION (Including special warning terms if applicable)
DREV	UNCLASSIFIED

3. TITLE (Its classification should be indicated by the appropriate abbreviation (S,C,R or U)
NUMERICAL DEVELOPMENT OF AN EQUIVALENT AXISYMMETRIC FSP

4. AUTHORS (Last name, first name, middle initial. If military, show rank, e.g. Doe, Maj. John E.)
NANDLALL, D.

5. DATE OF PUBLICATION (month and year)	6a. NO. OF PAGES	6b. NO. OF REFERENCES
March 96	22	4

7. DESCRIPTIVE NOTES (the category of the document, e.g. technical report, technical note or memorandum. Give the inclusive dates when a specific reporting period is covered.)
Technical Report

8. SPONSORING ACTIVITY (name and address)
PMO LAV 006, NDHQ Ottawa, K1A 0K2

9a. PROJECT OR GRANT NO. (Please specify whether project or grant)	9b. CONTRACT NO.

10a.ORIGINATOR'S DOCUMENT NUMBER	10b. OTHER DOCUMENT NOS.
R-9530	N/A

11. DOCUMENT AVAILABILITY (any limitations on further dissemination of the document, other than those imposed by security classification)
- [X] Unlimited distribution
- [ ] Contractors in appoved countries (specify)
- [ ] Canadian contractors (with need-to-know)
- [ ] Government (with need-to-know)
- [ ] Defence departments
- [ ] Other (please specify) :

12. DOCUMENT ANNOUNCEMENT (any limitation to the bibliographic announcement of this document. This will normally correspond to the Document Availability (11). However, where further distribution (beyond the audience specified in 11) is possible, a wider announcement audience may be selected.)

13. ABSTRACT (a brief and factual summary of the document. It may also appear elsewhere in the body of the document itself. It is highly desirable that the abstract of classified documents be unclassified. Each paragraph of the abstract shall begin with an indication of the security classification of the information in the paragraph (unless the document itself is unclassified) represented as (S), (C), (R), or (U). It is not necessary to include here abstracts in both official languages unless the text is bilingual).

In this study, an attempt is made to develop an equivalent axisymmetric fragment simulating projectile (FSP) using numerical simulations to represent a non-axisymmetric standard FSP for the development of calibration curves for witness packs. Three different axisymmetric FSP models were investigated. In the first model, the cutting edge perimeter of the true FSP was conserved. For the second and third models, the presented area of the true FSP on impact and the bevel angle were conserved respectively. The results obtained indicate that the third model yields the same ballistic limit as the standard non-axisymmetric FSP. However, it was found that the mode of the plug formation for the axisymmetric and non-axisymmetric models differs substantially.

14. KEYWORDS, DESCRIPTORS or IDENTIFIERS (technically meaningful terms or short phrases that characterize a document and could be helpful in cataloguing the document. They should be selected so that no security classification is required. Identifiers, such as equipment model designation, trade name, military project code name, geographic location may also be included. If possible keywords should be selected from a published thesaurus. e.g. Thesaurus of Engineering and Scientific Terms (TEST) and that thesaurus-identified. If it is not possible to select indexing terms which are Unclassified, the calssification of each sould be indicated as with the title.)

NUMERICAL SIMULATION, HYDROCODE, PENETRATION, WITNESS PACK, BEHIND-ARMOUR DEBRIS, HIGH STRAIN RATE, FRAGMENT, HIGH VELOCITY IMPACT.

498353